LAWRENCE
LIVERMORE
NATIONAL
LABORATORY

UCRL-JRNL-225608

New Phases of Hydrogen-Bonded Systems at Extreme Conditions

M. R. Manaa, N. Goldman, L. E. Fried

October 25, 2006

Phase Transition

Disclaimer

New Phases of Hydrogen-Bonded Systems at Extreme Conditions

M. R. MANAA*, N. GOLDMAN and L. E. Fried

University of California, Lawrence Livermore National Laboratory, Livermore, California 94551, USA

*Corresponding author. Email: manaa1@llnl.gov

Abstract

We study the behavior of hydrogen-bonded systems under high-pressure and temperature. First principle calculations of formic acid under isotropic pressure up to 70 GPa reveal the existence of a polymerization phase at around 20 GPa, in support of recent IR, Raman, and XRD experiments. In this phase, covalent bonding develops between molecules of the same chain through symmetrization of hydrogen bonds. We also performed molecular dynamics simulations of water at pressures up to 115 GPa and 2000 K. Along this isotherm, we are able to define three different phases. We observe a molecular fluid phase with superionic diffusion of the hydrogens for pressure 34 GPa to 58 GPa. We report a transformation to a phase dominated by transient networks of symmetric O-H hydrogen bonds at 95 - 115 GPa. As in formic acid, the network can be attributed to the symmetrization of the hydrogen bond, similar to the ice VII to ice X transition.

Keywords: Polymeric Formic Acid; Superionic Water; Hydrogen Bonding; Ab initio Simulations; High-Pressure Phases.

1. INTRODUCTION

Hydrogen bonding is ubiquitous in many fundamental chemical and biological systems. From water, in its both solid and liquid phases, to nucleic acid base pairs, hydrogen bonding is an integral part in understanding the structural, chemical and physical attributes of these systems. External perturbations of high-pressure and high-temperature can lead to ordered (disordered) enhancement in systems prone to strong hydrogen bonding, with important implications to astrochemical and planetary processes. Advances in diamond anvil cell (DAC), and the application of first-principles molecular dynamic (MD) methods in the last few years have provided profound insight into the nature of hydrogen bonding of materials at high-pressure. Two recent studies of discovering (1) polymerization in formic acid, the simplest carboxylic acid, and (2) superionic phase in water are presented as prime examples of hydrogen bonded systems at extreme conditions.

At first, we examine the behaviour of formic acid (HCOOH) under isotropic compression of up to 70 GPa. As the simplest of carboxylic acids, formic acid is a hydrogen-bonded cyclic dimer in the gas-phase. [1] Thanks to its two hydrogen bond acceptor sites, the hydroxyl and formyl sites, which, combined with its two oxygen acceptor sites provide several possibilities for hydrogen bonds formation. [2] Under high-pressure, hydrogen bonds association at these sites offer a rich opportunity to probe several important phenomena such as bond geometry and strength, proton transfer [3], and polymerization. In its solid form, formic acid consists of infinite chains of hydrogen-bonded molecules with two conformations: *cis* and *trans* (see figure 1).

The low–temperature solid consists of the *cis* conformation [4], with anticipated transformations to mixed *cis-trans,* proton disordered [5], or pure trans phase [6] at elevated temperature and pressure. Under pressure, however, several studies reported transformation of the crystal structure from that at ambient pressure and low temperature. According to single-crystal x-ray diffraction (XRD) study [7], formic acid formed near dimers consisting of *cis*- and *trans*- molecules. A Raman study performed on deuterated formic acid, DCOOD, reported softening of O-D and C=O stretch bands, which indicate strengthening of the hydrogen bond. [6] A change of slope of these bands at 4.5 GPa was interpreted as the phase transformation related to the conformational change from *cis* to *trans.* The most recent combined x-ray powder diffraction and IR-absorption study [8] confirmed the initial softening of O-H and C=O bonds and the frequency anomalies at 4.5 GPa, but finds the crystal structure the same as the one at low temperature [4] and unchanged to 12 GPa. The more recent XRD, Raman, and IR experiments of Goncharove et al. [9] revealed that the low-temperature $Pna2_1$ structure of formic acid is stable at room temperature up to 35-40 GPa. It was found that at pressure around 20 GPa the conformer distinction disappears, and the emergence of symmetric hydrogen bonding is manifested. Still, at higher pressure a gradual transformation amorphous phase occurs. The transformation showed a large hysteresis on pressure release, reverting the initial phase at 5 GPa.

Secondly, we discuss the transformation of water to the superionic solid phase at high-pressure and temperature. Superionic solids are compounds that exhibit exceptionally high ionic conductivity, where one ion type diffuses through a crystalline lattice of the remaining types. This is a unique phase of matter in which chemical bonds are breaking and reforming very rapidly. Since their discovery in 1836, a fundamental understanding of superionic conductors has been one of the major challenges in condensed matter physics. [10] In general, it has been difficult to create a simple set of rules governing superionic phases. Studies have mostly been limited to metal based compounds, such as metal halides AgI and PbF_2. [10] However, the existence of superionic solid phases of hydrogen-bonded compounds had been theorized previously. [11,12]

Recent experimental and computational results indicate the presence of a high-pressure triple point in the H_2O phase diagram [13-15], including a so-called superionic solid phase with fast hydrogen diffusion. [15,16] Goldman et al. have recently described the emergence of symmetric hydrogen bonding in superionic water at 2000 K and 95 GPa. In symmetric hydrogen bonding, the intramolecular X-H bond becomes identical to the intermolecular X-H bond, where X is an electronegative element. It has been suggested that for superionic solids a mixed ionic/covalent bonding character stabilizes the mobile ion during the diffusion process. Symmetric hydrogen bonding provides mixed ionic/covalent bonding, and thus could be a key factor in superionic diffusion in hydrogen bonding systems. This represents an entirely novel approach for creating a simple physical description of superionic solids. Symmetric hydrogen bonding has been observed in other hydrides, including HF [17,18], DCl [19], and HBr. [20]

2. FORMIC ACID UNDER PRESSURE

The recent combined IR, Raman, and XRD experiments of Goncharove et al. [9] to pressure up to 50 GPa have revealed several interesting facts. The IR absorption spectra showed a number of fundamentals, with the O-H band exhibiting a pronounced softening and broadening. The pressure dependence of the O-H stretch mode resulted in a transition pressure (16 GPa) that corresponds to the O-H mode instability. The Raman measurements showed substantial broadening in the C-O and C=O stretching modes, as well as in the O=C-O bending mode in the pressure range of 10-25 GPa. In the pressure range of 38-45 GPa, narrow Raman bands of the molecular phase were superseded by broad bands indicating a loss of a long-range order. XRD patterns also showed a gradual appearance of diffuse bands, characteristic of a highly disordered state.

In order to determine structural changes, we performed ab initio density functional calculations on crystal formic acid under isotropic pressure up to 70 GPa, and compared with experimental results when possible. The calculations implemented the spin-polarized generalized gradient corrected approximation of Perdew -Wang (PW91) [21] for the exchange-correlation potential. Electron-ion interactions were described by Vanderbilt-type ultrasoft pseudopotentials, [22] and valence orbitals were expanded in a plane wave basis set with a kinetic energy cutoff of 380 eV. Total energy convergence was 0.02 meV/atom. Stresses on the unit cell, including a term for applied external stresses, were calculated and used in the geometry optimization procedure. We also performed constant volume and temperature (T=298 K), Born-Oppenheimer molecular dynamics (MD) simulations of 5 ps duration to obtain a power spectrum at low pressure to compare with experimental Raman results.

Figure 2a displays the results of calculated pressure versus reduced volume up to 70 GPa, while figure 2b compare these results with those of XRD experiments in their respective pressure range. We obtained a low-pressure (1GPa) power spectrum from an MD simulation that is in very good agreement with the Raman study. [9] As shown in figure 2, we find that the experimentally and theoretically determined unit cell volumes agree very well above pressure of 10 GPa, but somewhat deviate at lower pressure. This could be attributed to convergence criteria in the optimization procedure, and more stringent criteria should produce better agreement. Both XRD experiments, however, are in good agreement up to 12 GPa. Further, Deviation from XRD experimental results is also exhibited in the variation of the reduced lattice constant *b* with pressure as shown in Figure 3. Here, we note that while quantitative agreement with experiment is produced for the *a* and *c* constants, the deviation for the parameter *b* is up to 10% from experiment, although the qualitative trend with pressure is maintained.

Figure 4 shows the calculated pressure dependence of both the inter- and intra-molecular O-H bonds. The intra-molecular bond distance shows the initial increase of O-H with pressure, in agreement with the soft mode behaviour found experimentally. [9] At about 21 GPa, the two curves cross and a transition of sort appears. This critical point represents the symmetrization of the hydrogen bond. Experimentally, this transition pressure of the O-H was determined to occur at 16 GPa, from fitting the observed pressure dependence in the Raman spectra of the O-H stretch soft mode. [9]

Formic acid with symmetric hydrogen bonds is a linear chain polymer. Theoretical calculations provide an insight into this polymerization state. At low pressure (1.4 GPa), formic acid exhibit distinct C=O and C-O bonds that correspond to sp^2 and sp^3 hybridization, respectively. At this pressure, the bond lengths are R(C=O) = 1.24Å and R(CO) =1.30Å, which compare well with those determined from X-rays at ambient conditions, R(C=O) = 1.23Å and R(CO) =1.36Å. [23] As pressure increase, a polymeric chain network develops along the *b* and *c* planes due to a substantial hydrogen bonding contribution and transformation in the C=O bond character. As the O-H bonds decrease, a significant electronic density reorganization occurs in the O-C=O bonds, eventually leading to sp^2 and sp^3 transition, and both bonds become almost equivalent in length. This eliminates the distinction between the single and double C-O bonds, consistent with the observed merging of the C-O and C=O bands. Since in the polymeric phase individual molecules do not exist, the *cis-trans* conformational differences vanish. Further, Computational results show that the Mulliken bond order for the O-H hydrogen bonds at pressure of 38 GPa is about 0.3-0.4, which indicates a substantial covalent contribution. These calculations at low (P=1.4 GPa) and high (P=38 GPa) pressure clearly demonstrate the bond reorganization as shown below.

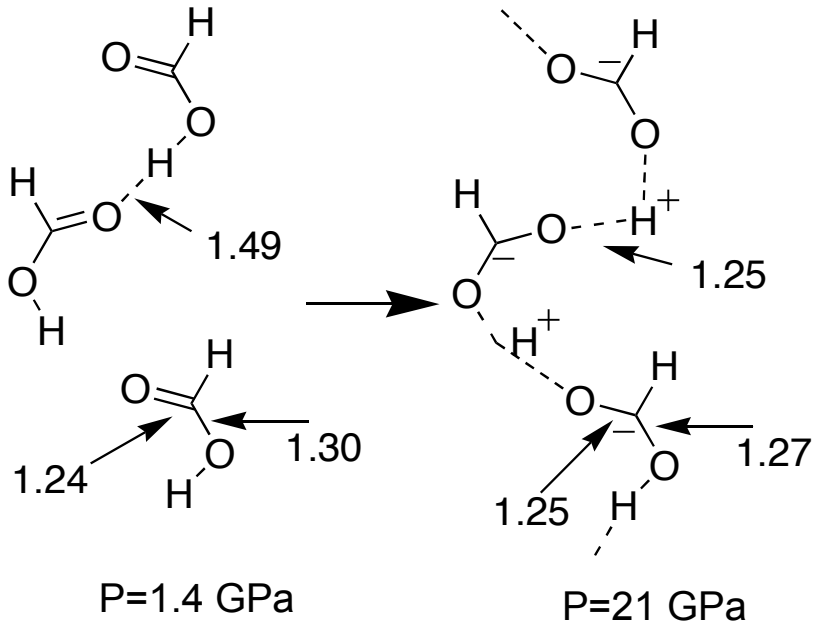

3. SIMULATIONS OF WATER AT EXTREME CONDITIONS

The density profiles of large planets, such as Uranus and Neptune, suggest that there exists within a thick layer of "hot ice", which is thought to be 56% H_2O, 36% CH_4, and 8% NH_3. [24] This has lead to theoretical investigations of the water phase diagram [11], in which Car-Parrinello Molecular Dynamics (CPMD) simulations [25] were conducted at temperature and pressures ranging from 300 to 7000 K and 30-300 GPa. [12] At temperatures above 2000 K and pressures above 30 GPa, there was observed a superionic phase in which the oxygen atoms had formed a bcc lattice, and the hydrogen atoms diffused extremely rapidly (ca.10^{-4} cm^2/s) via a hopping mechanism between oxygen lattice sites. Experimental results for the ionic conductivity of water at similar state conditions [26,27] agree well with the results from Ref. [12], confirming the idea of a superionic phase, and indicating a complete atomic ionization of water molecules under extreme conditions (P > 75GPa, T > 4000 K). [27]

More recent *ab initio* MD simulations were performed at temperatures up to 2000 K and pressures up to 30 GPa. [28, 29] Under these conditions, it was found that the molecular ions H_3O^+ and OH^- are the major charge carriers in a fluid phase, in contrast to the bcc crystal predicted for the superionic phase. The fluid high-pressure phase has been recently confirmed by X-ray diffraction results of water melting at ca. 1000 K and up to 40 GPa pressure. [30-32] In addition, extrapolations of the proton diffusion constant of ice into the superionic region were found to be far lower than a superionic criteria of 10^{-4} cm^2/s. [33] Thus, it is clear there is great need for further work to resolve the apparently conflicting data.

We have investigated the superionic phase with more extensive first principles Car-Parrinello molecular dynamics simulations. [16] Calculated power spectra (i. e., the vibrational density of states, or VDOS) have recently been compared to measured experimental Raman spectra at pressures up to 55 GPa and temperatures of 1500 K. [15] The agreement between theory and experiment was very good. In particular, weakening and broadening of the OH stretch mode at 55 GPa was found both theoretically and experimentally. A summary of our results on the phase diagram of water is shown in Figure 5.

For our simulations, we used the CPMD code v.3.91, with the BLYP exchange-correlation functional,[34,35] and Troullier-Martins pseudo-potentials [36] for both oxygen and hydrogen. A planewave cutoff of 120 Ry was employed to insure convergence of the pressure, although all other properties were seen to converge with a much lower cutoff (85 Ry). The system size was 54 H_2O molecules. The temperature was controlled by using Nosé-Hoover thermostats for all nuclear degrees of freedom. [37] We chose electron mass of 200 a.u. and a time step of 0.048 fs.

Initial conditions were generated in two ways: 1) a liquid configuration at 2000 K was compressed from 1.0 g/cc to the desired density in sequential steps of 0.2 g/cc from an equilibrated sample. 2) An ice VII configuration was relaxed at the density of interest, then heated to 2000 K in steps of 300 degrees each, for a duration of 0.5 - 1 ps. For convenience, we will refer to the first set of simulations as the "L" set, and the second as the "S" set. Unless stated otherwise, the results (including the pressures) from the "S" initial configurations are those reported. Once the desired density and/or temperature were achieved, all simulations were equilibrated for a minimum of 2 ps. Data collection simulations were run from 5-10 ps.

The calculated diffusion constants of hydrogen and oxygen atoms are shown in Figure 6, and the inset plot shows the equation of state for this isotherm for both "L" and "S" simulations. The two results are virtually identical up until 2.6 g/cc. At 34 GPa (2.0 g/cc), the hydrogen atom diffusion constant has achieved values associated with superionic conductivity (greater than 10^{-4} cm^2/s). The diffusion constant remains relatively constant with increasing density, in qualitative agreement with the experimental results of Chau et al. for the ionic conductivity.[27]

On the other hand, the O diffusion constant drops to zero at 75 GPa (2.6 g/cc) for both "L" and "S" initial configurations. The surprisingly small hysteresis in the fluid to superionic transition allows us to place the transition point between 70 GPa (2.5 g/cc) and 75 GPa (2.6 g/cc). Our transition pressure of 75 GPa is much higher than the value of 30 GPa predicted earlier.[12] This is likely due to their use of a much smaller basis set (70 Ry). Our results are in disagreement with simple extrapolations of the proton diffusion constant to high temperatures. [33]

Radial distribution functions (RDFs) for the "S" simulations are shown in Figure 7. Analysis of the oxygen-oxygen RDF for all pressures yields a coordination number of the first peak of just over 14, consistent with a high-density bcc lattice in which the first two peaks are broadened due to thermal fluctuations. We also find that in the pressure range 75 - 115 GPa, the bcc lattice undergoes large amplitude vibrations, even though the RDF's in Figure 7 have width similar to that of a liquid or a glass. Examination of the O-O and H-H RDFs indicate that no O-O or H-H covalent bonds are formed during the simulations at all densities.

We observe a shift of the first minimum of the O-H RDF from 1.30Å at 34 GPa to 1.70Å at 115 GPa. This bears a strong resemblance to the ice VII to ice X transition in which the covalent O-H bond distance of ice becomes equivalent to the hydrogen bond distance as pressure is increased. However, the superionic phase differs from ice X, in that the position of the first peak in $g(R_{OH})$ is not half the distance of the first O-O peak.[38]

We have also analyzed species lifetimes. Above 2.6 g/cc, the lifetime of all species is less than 12 fs, which is roughly the period of an O-H bond vibration (ca. 10 fs). Hence, water above 75 GPa and at 2000 K does not contain any molecular states, but instead forms a collection of short-lived "transient" states. The "L" simulations at 2.6 g/cc (77 GPa) and 2000 K yield lifetimes nearly identical to that found in the "S" simulations described above (within 0.5 fs). This indicates that the amorphous states formed from the "L" simulations are closely related to the superionic bcc crystal states found in the "S" simulations. At pressures of 95 and 115 GPa, the increase in the O-H bond distance leads to the formation of extensive bond networks (Figure 8). These networks consist entirely of O-H bonds, while O-O and H-H bonds were not found to be present at any point.

4. CONCLUSION

Formic acid and water represent two prime examples to probe novel phase transitions in hydrogen-bonded systems at elevated conditions of pressure and temperature. Our first principles calculations of these two systems reveal several new findings that are supported by recent Raman, IR, and XRD experimental investigations. For formic acid, our calculations of this system under isotropic pressure up to 70 GPa demonstrate the existence of a polymerization phase starting at around 20 GPa, where covalent bonding develops between molecules of the same chain through symmetrization of hydrogen bonds. Our simulations of water at pressures up to 115 GPa (3.0 g/cc) and 2000 K reveal three different phases along this isotherm. First, from 34 GPa to 58 GPa (2.0-2.4 g/cc), we observe a molecular fluid phase with superionic diffusion of the hydrogens. Second, at 75 GPa (2.6 g/cc), we find a stable bcc oxygen lattice with superionic proton conduction. O-H bonds within this "solid" phase are found to be mostly covalent, despite their exceedingly short lifetimes of ca. 10 fs. Third, at 95 - 115 GPa (2.8 - 3.0 g/cc) we find a transformation to a phase dominated by transient networks of symmetric O-H hydrogen bonds. The network can be attributed to the symmetrization of the hydrogen bond, similar to the ice VII to ice X transition.

Acknowledgments:

This work was performed under the auspices of the U.S. Department of Energy by UC, Lawrence Livermore National Laboratory under contract number W-7405-Eng-48.

Figure Caption

FIGURE 1: The cis (a) and trans (b) polymorphic forms of crystalline HCOOH.

FIGURE 2: (a) Calculated pressure as a function of reduced volume. (b) Calculated and experimental relation of unit cell volume as a function of pressure.

FIGURE 3: Reduced lattice constants as a function of pressure for formic acid: calculated in this work (gray lines and symbols), and XRD experimental results of Ref.9 (black lines and symbols).

FIGURE 4: Calculated pressure dependence of the O-H inter and intra-molecular bond distances (in Å) in formic acid.

FIGURE 5: The phase diagram of H_2O as measured experimentally [15] (black) and through first principles simulations (red and green colored). [15, 16]

FIGURE 6: Diffusion constants for O and H atoms at 2000 K as a function of density. The lines with circles correspond to hydrogen, and the lines with squares to oxygen. The solid lines correspond to a liquid ("L") initial configuration, and the dashed lines to an ice VII ("S") initial configuration. The inset plot shows the pressure as a function of density at 2000 K, where the triangles correspond to "L" and the X's to "S".

FIGURE 7: O-H radial distribution function as a function of density. At 34 GPa we find a fluid state. At 75 GPa we show a "covalent" solid phase. At 115 GPa, we find a "network" phase with symmetric hydrogen bonding.

FIGURE 8: Snapshots of the simulations at 75 GPa and 115 GPa. At 75 GPa, the water molecules are starting to cluster, and at 115 GPa, a well-defined network has been formed. The protons dissociate very rapidly and form new clusters (at 75 GPa) or networks of bonds (at 115 GPa).

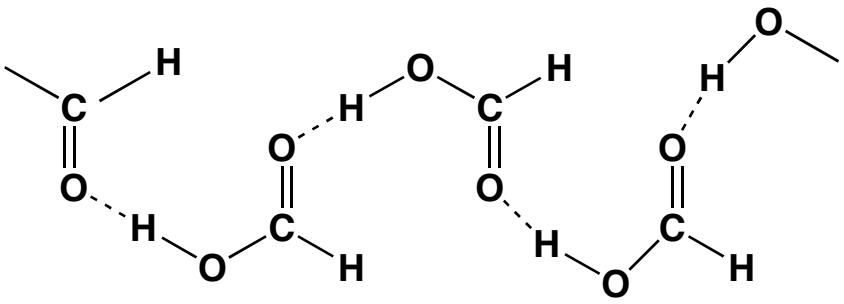

(a)

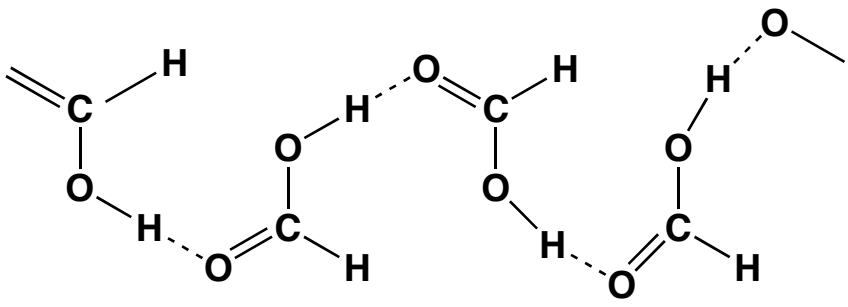

(b)

Figure 1.

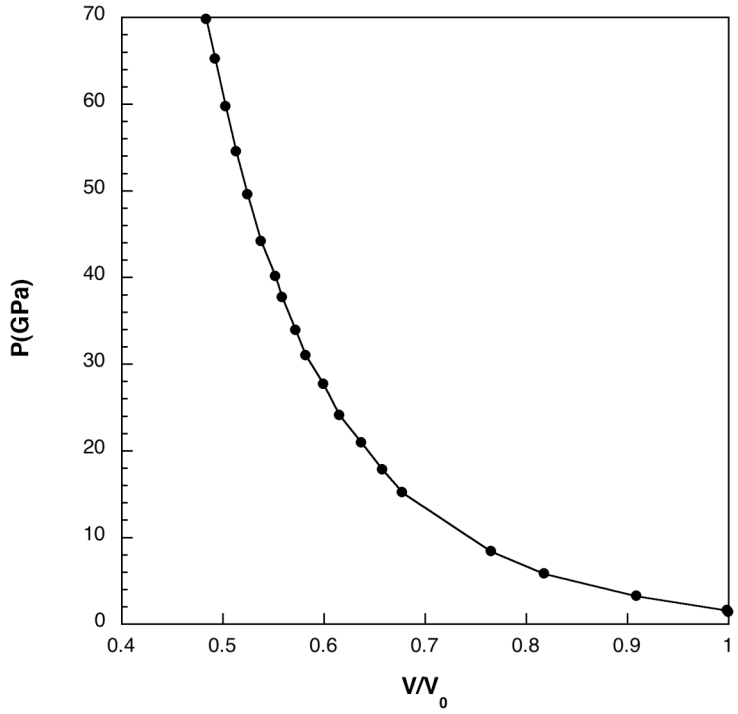
P(GPa)
V/V0
70
60
50
40
30
20
10
0
0.4
0.5
0.6
0.7
0.8
0.9
1

(a)

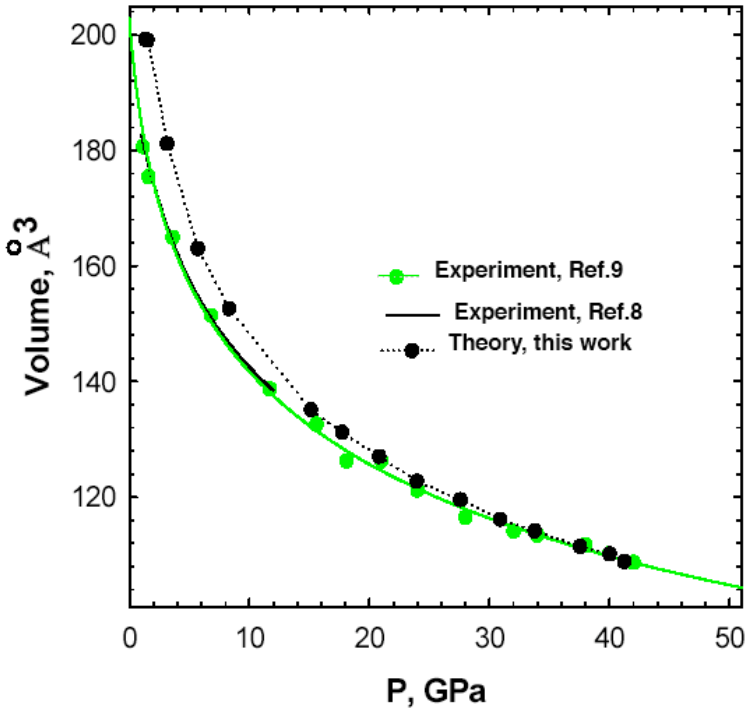
Volume, Å3
P, GPa
Experiment, Ref.9
Experiment, Ref.8
Theory, this work
200
180
160
140
120
0
10
20
30
40
50

(b)

Figure 2.

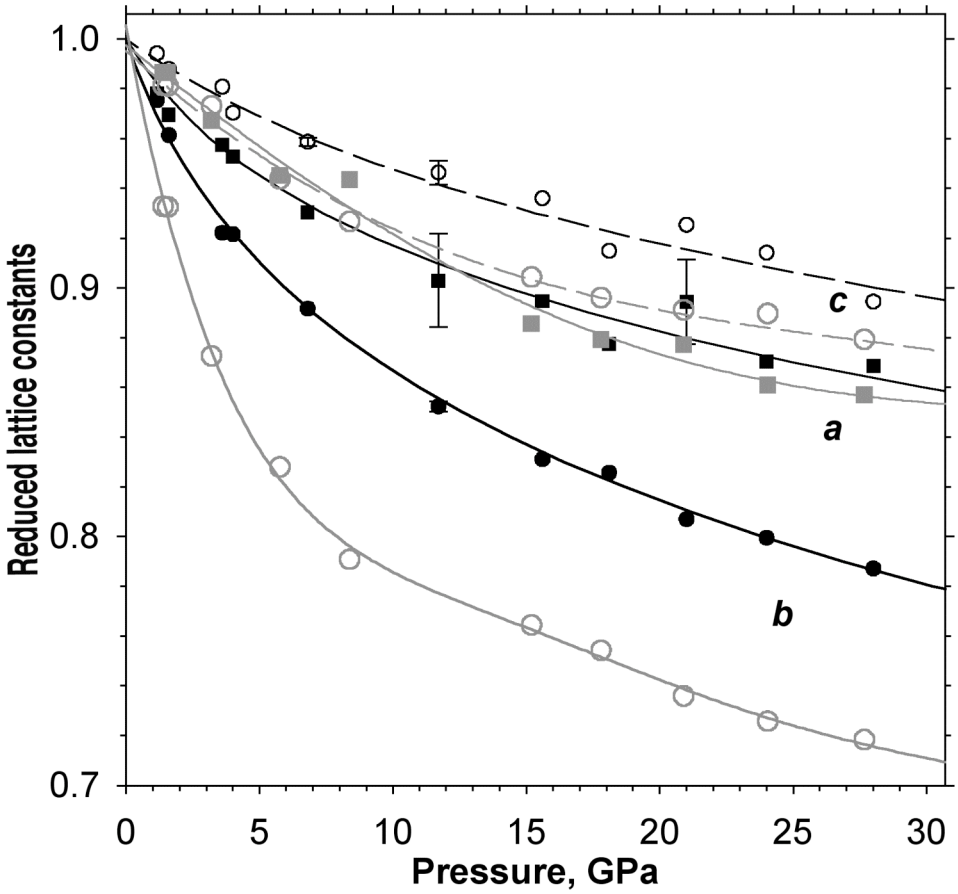
1.0
0.9
0.8
0.7
Reduced lattice constants
0
5
10
15
20
25
30
Pressure, GPa
c
a
b

Figure 3.

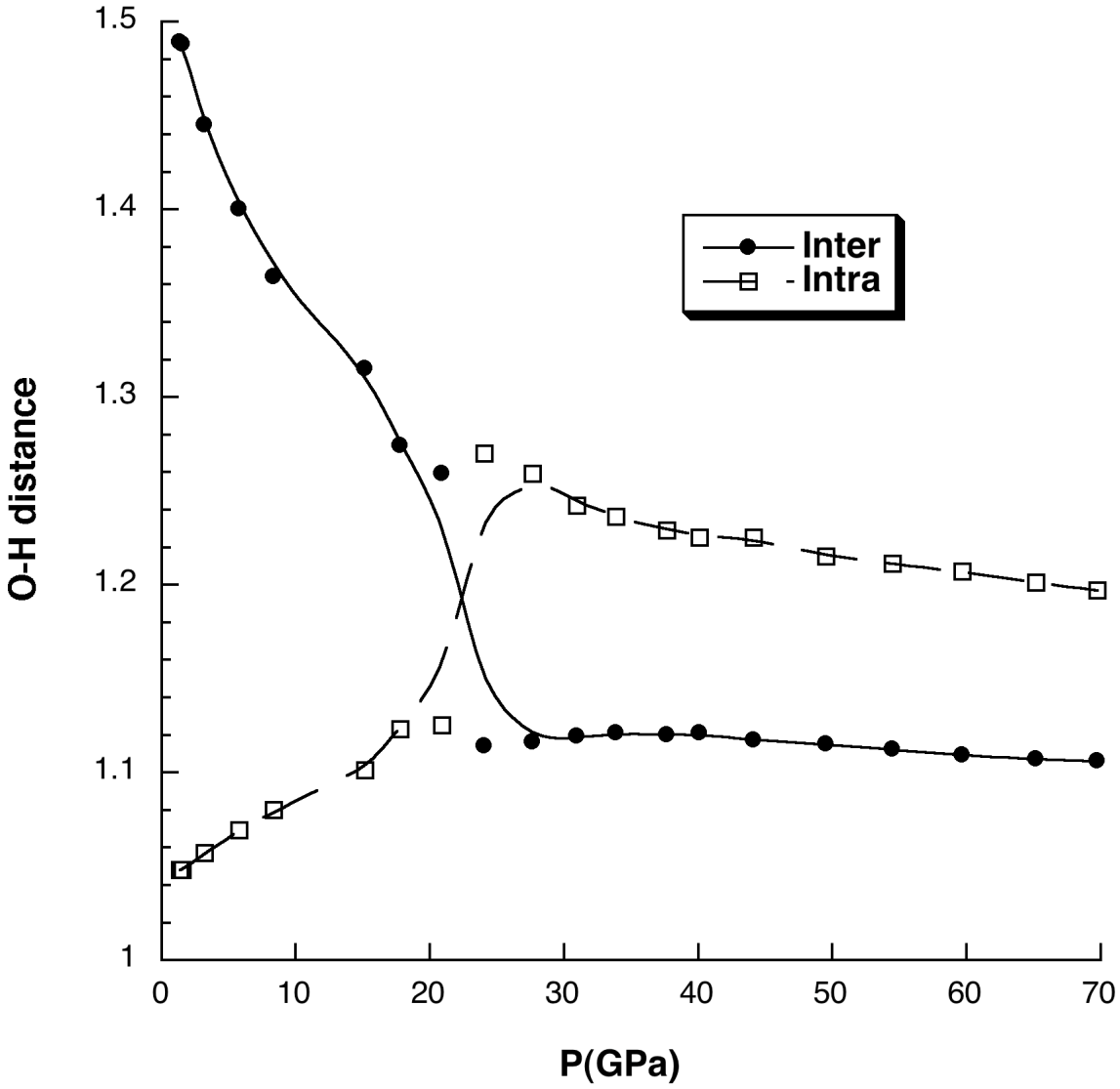
1.5
1.4
1.3
1.2
1.1
1
O-H distance
Inter
Intra
0
10
20
30
40
50
60
70
P(GPa)

Figure 4.

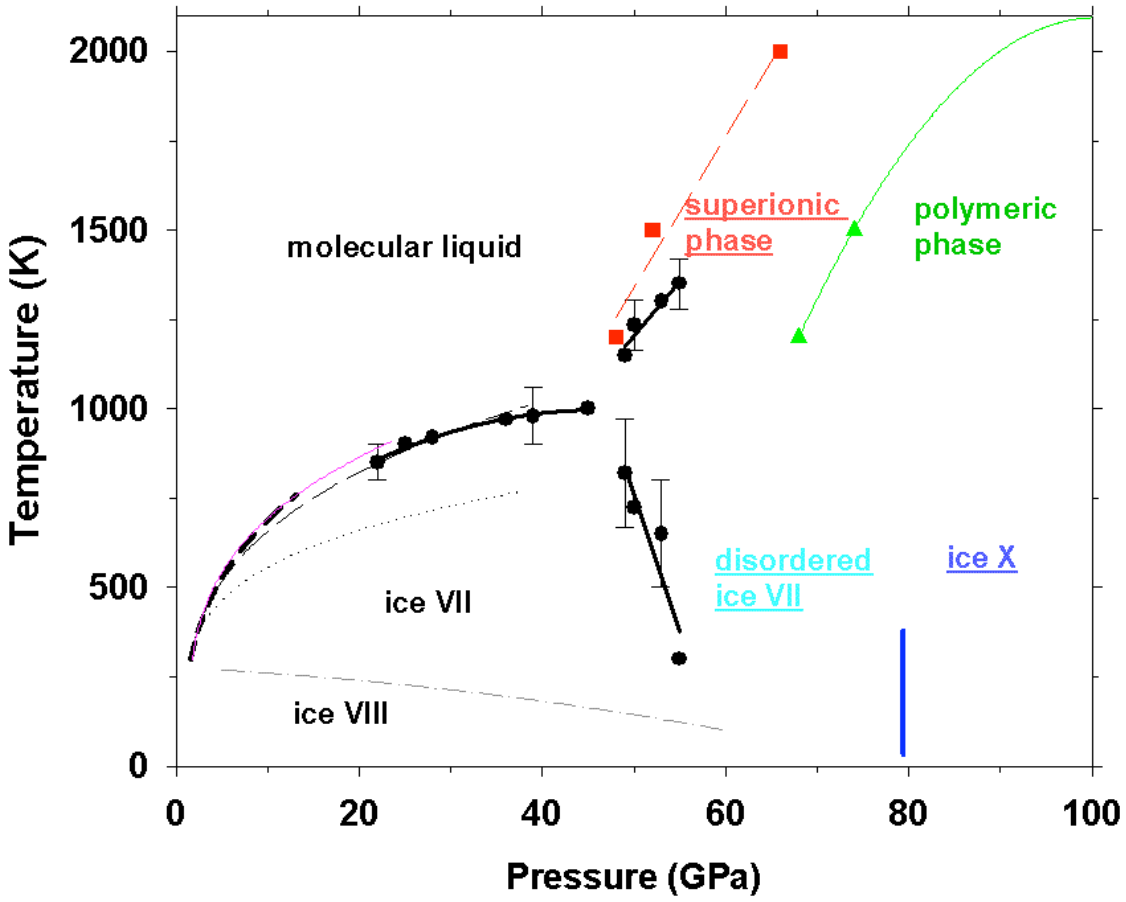
2000
1500
1000
500
0
Temperature (K)
0
20
40
60
80
100
Pressure (GPa)
molecular liquid
superionic
phase
polymeric
phase
ice VII
ice VIII
disordered
ice VII
ice X

Figure 5.

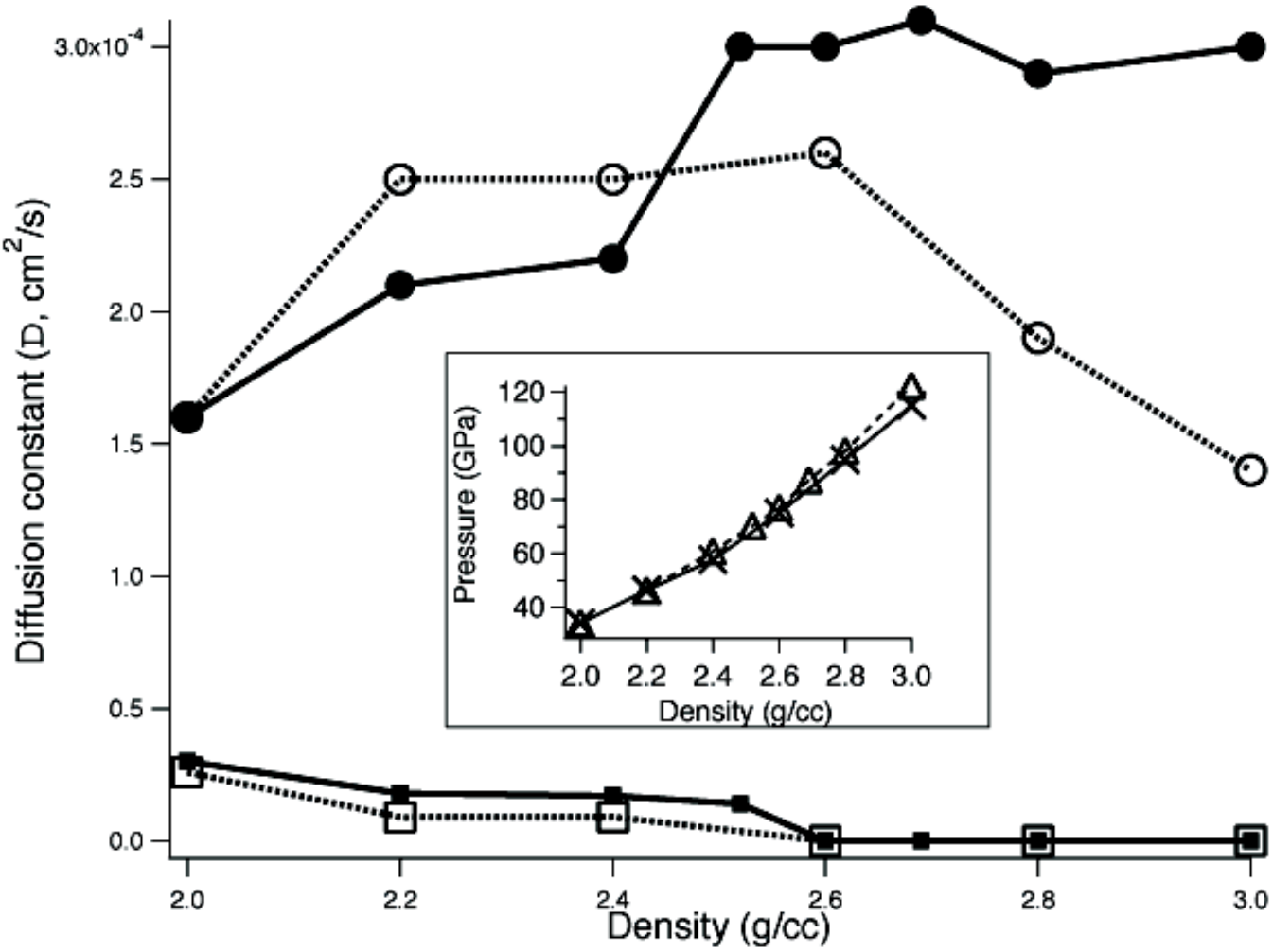
3.0x10^-4
2.5
2.0
1.5
1.0
0.5
0.0
Diffusion constant (D, cm^2/s)
2.0
2.2
2.4
2.6
2.8
3.0
Density (g/cc)
120
100
80
60
40
Pressure (GPa)
2.0 2.2 2.4 2.6 2.8 3.0
Density (g/cc)

Figure 6.

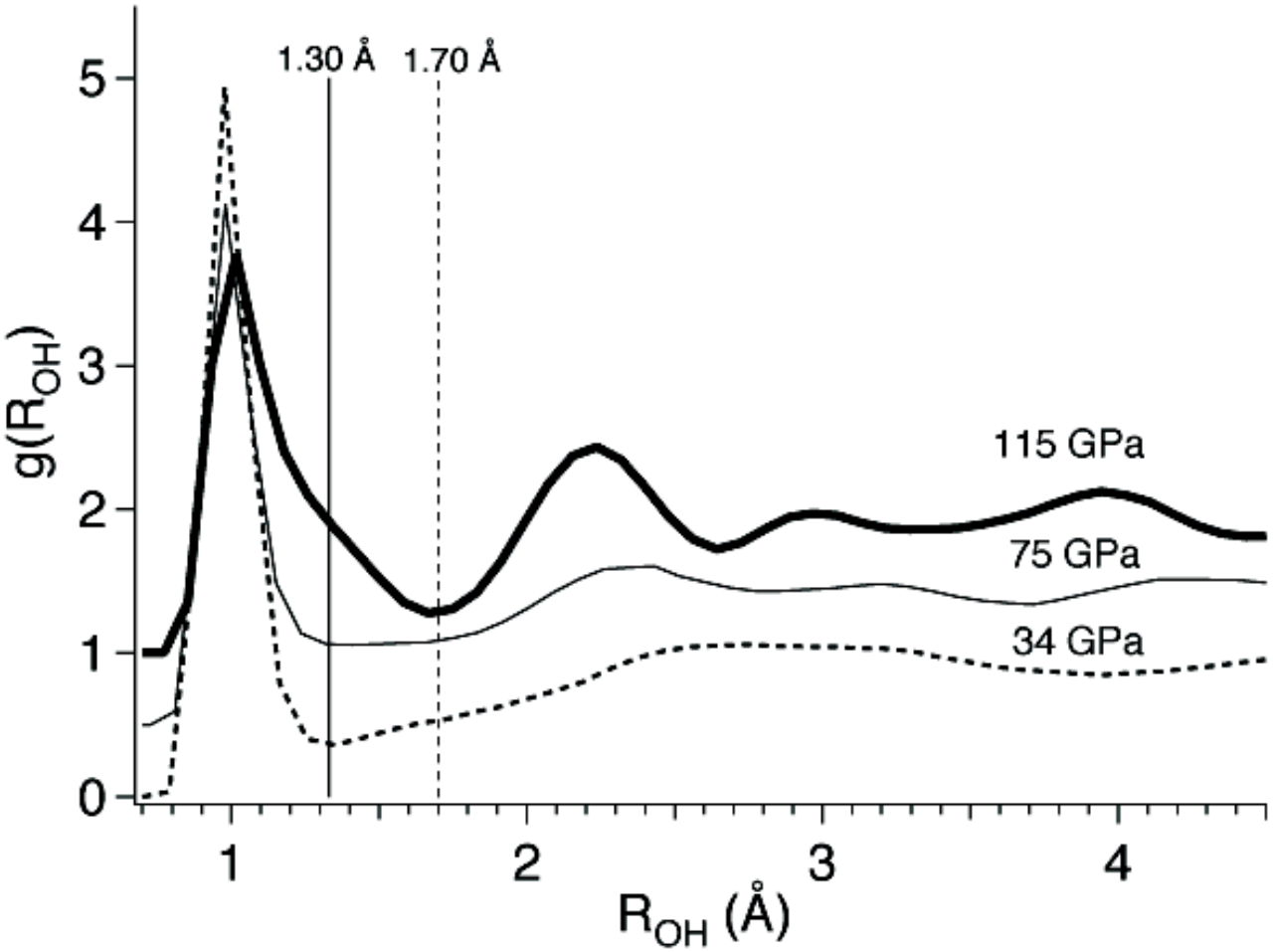

Figure 7.

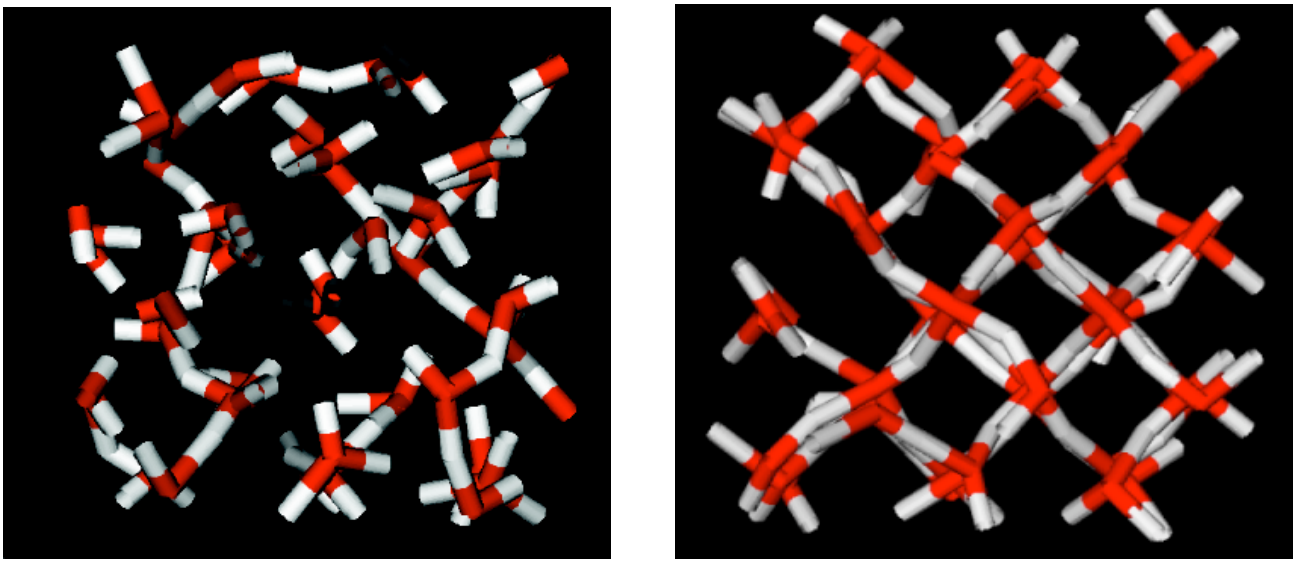

Figure 8.

REFERENCES:

[1] G. Kwei, R. Curl, J. Chem. Phys. **32,** 1592 (1960).
[2] P. Mináry, P. Jedlovszky, M. Mezei, and L. Turi, J. Phys. Chem. B **104**, 8287 (2000).
[3] G. N. Robertson and M. C. Lawrence, Chem. Phys. **62**, 131 (1981).
[4] I. Nahringbauer, Acta Crystallogr., B **34**, 315 (1978**)**.
[5] H. R. Zelsmann, F. Bellon, Y. Mareshal, and B. Bullemer, Chem. Phys. Lett. **6**, 513 (1970).
[6] H. Shimizu, Physica **139&140B**, 479 (1986).
[7] D. R. Allan and S. J. Clark, Phys. Rev. Lett. **82**, 3464 (1999).
[8] H. Yamawaki *et al*., in *Science and Technology of High Pressure*, edited by M. H. Manghnani, W. J. Nellis, and M. Nicol (Universities Press, Hyderabad, India, 2000), pp. 125-128.
[9] A. F. Goncharov, M. R. Manaa, J. M. Zaug, *et al*. Phys. Rev. Lett. **94**, 065505 (2005).
[10] S. Hull, Rep. Prog. Phys., **67**, 1233-1314 (2004).
[11] P. Demontis, R. LeSar, and M. L. Klein, Phys. Rev. Lett., **60**, 2284 (1988).
[12] C. Cavazzoni, G. L. Chiarotti, S. Scandolo, *et al*., Science, **283**, 44-46 (1999).
[13] B. Schwager, L. Chudinovbskikh, and R. Boehler, J. Phys.: Condens. Matter, **16**, 1177 (2004).
[14] J. –F. Lin, E. Gregoryanz, V. V. Struzhkin, *et al*., Geophys. Res. Lett., **32**, 11306 (2005).
[15] A. F. Goncharov, N. Goldman, L. E. Fried, *et al*., Phys. Rev. Lett., **94**, 125508 (2005).
[16] N. Goldman, L. E. Fried, *et al*., Phys. Rev. Lett., **94**, 217801 (2005).
[17] N. Goldman, and L. E. Fried, J. Chem. Phys., **125**, 044501 (2006).
[18] D. A. Pinnick, A. I. Katz, and R. C. Hanson, Phys. Rev. B, **39**, 8677 (1989).
[19] E. Katoh, H. Yamawaki, *et al*., Phys. Rev. B, **61**, 119 (2000).
[20] T. Ikeda, M. Sprik, *et al*., J. Chem. Phys., **111**, 1595-1607 (1999).
[21] J. P. Perdew and Y. Wang, Phys. Rev. B **46,** 6671 (1992).
[22] D. Vanderbilt, Phys. Rev. B **41,** 7892 (1990).
[23] A. Albinati, K. D. Rouse, and M. W. Thomas, Acta Crystallogr. Sect. B **34**, 2188 (1978).
[24] W. B. Hubbard, Science, **214**, 145 (1981).
[25] R. Car, and M. Parrinello, Phys. Rev. Lett, **55**, 2471 (1985).
[26] W. J. Nellis, N. C. Holmes, A. C. Mitchell, *et al*., J. Chem. Phys, **107**, 9096 (1997).
[27] R. Chau, A. C. Mitchell, R. W. Minich, and W. J. Nellis, J. Chem. Phys, **114**, 1361 (2001).
[28] E. Schwegler, G. Galli, F. Gygi, and R. Q. Hood, Phys. Rev. Lett., **87**, 265501 (2001).
[29] C. Dellago, P. L. Geissler, D. Chandler, *et al*., Phys. Rev. Lett., **89**, 199601 (2001).
[30] B. Schwager, L. Chudinovskikh, A. Gavriliuk, and R. J. Boehler, J. Phys: Condensed Matter, **16**, S1177 (2004).
[31] M. Frank, Y. Fei, and J. Z. Hu, Geochemica et Cosmochimica Acta, **68**, 2781 (2004).
[32] J. F. Lin, B. Militzer, V. V. Struzhkin, *et al*., J. Chem. Phys., **121**, 8423-8427 (2004).
[33] E. Katoh, H. Yamawaki, H. Fujihisa, *et al*., Science, **295**, 1264 (2004).
[34] A. D. Becke, Phys. Rev. A, **38**, 3098 (1988).
[35] C. Lee, W. Yang, and R. G. Parr, Phys. Rev. B, **37**, 785 (1988).
[36] N. Troullier, and J. Martins, Phys. Rev. B, **43**, 1993 (1991).
[37] W. G. Hoover, Phys. Rev. A, **31**, 1695 (1985).
[38] M. Benoit, A. H. Romero, and D. Marx, Phys. Rev. Lett., **89**, 145501-1 (2002).